Lagrangian chaos and particle diffusion in electroconvection of planar nematic liquid crystals

Yoshiki Hidaka,[1,*] Megumi Hashiguchi,[1] Noriko Oikawa,[2] and Shoichi Kai[1]
[1]*Department of Applied Quantum Physics and Nuclear Engineering, Faculty of Engineering, Kyushu University, Fukuoka 819-0395, Japan*
[2]*Department of Physics, Graduate School of Science and Engineering, Tokyo Metropolitan University, Tokyo 192-0397, Japan*
(Received 6 March 2015; published 15 September 2015)

Two types of spatiotemporal chaos in the electroconvection of nematic liquid crystals, such as defect turbulence and spatiotemporal intermittency, have been statistically investigated according to the Lagrangian picture. Here fluctuations are traced using the motion of a single particle driven by chaotic convection. In the defect turbulence (fluctuating normal rolls), a particle is mainly trapped in a roll but sometimes jumps to a neighboring roll. Its activation energy is then obtained from the jumping (hopping) rate. This research clarifies that diffusion in the defect turbulence regime in electroconvection can be regarded as a kind of hopping process. The spatiotemporal intermittency appears as a coexistent state of ordered grid domains and turbulent domains. The motion of a single particle shows weak and strong diffusion, respectively, in the ordered and turbulent domains. The diffusion characteristics intermittently change from one to another with certain durations as the domains change. This research has found that the distribution function of the duration that a particle remains in an ordered area has a power-law decay for which the index is different from that obtained by the Eulerian measurement.

DOI: 10.1103/PhysRevE.92.032909 PACS number(s): 05.45.Jn, 05.40.−a, 47.27.−i

I. INTRODUCTION

Spatiotemporal chaos is a kind of weak turbulence in nonlinear dissipative systems that is characterized by the coexistence of order and disorder in space and time [1]. In other words, the system can be characterized by macroscopic fluctuations. To understand the system, therefore, it is necessary to clarify the properties of fluctuations from statistical mechanical viewpoints. Historically, such research has been conducted for thermal fluctuations and for fully developed turbulent fluctuations [2]. Various transport coefficients and energy transport spectra have then been obtained. For spatiotemporal chaos, there are difficulties in clarifying even the statistical mechanical properties of fluctuations, because they show the coexistence of order and disorder and nonuniformly distributed fluctuations. Systems that contain such spatiotemporal chaos are called mesoscopic fluctuation systems.

Research on spatiotemporal chaos has been mainly based on the Eulerian picture using order parameters [3]. However, transport properties of chaotic fluctuations are closely related to the Lagrangian picture using particle motion [4–7]. Furthermore, the Lagrangian picture, compared with the Eulerian picture, provides different information about the fluctuations. Chaotic behavior appearing only in the Lagrangian picture is called Lagrangian chaos or chaotic advection. For fully developed turbulence, information essential to determining the transport properties can be obtained from the mixing motion of many particles. For spatiotemporal chaos, however, the observation of the average behavior of particles is insufficient, because the coexistence of order and disorder mentioned above appears to create complex dynamics. We have thus experimentally investigated the statistical mechanical properties of spatiotemporal chaos occurring in electroconvective systems of a nematic liquid crystal from the motion of a single particle driven by chaotic advection, i.e., nonthermal Brownian motion [8].

The electroconvection of nematic liquid crystals involves various types of spatiotemporal chaos owing to the nonlinear interaction between the nematic director and convective flow [9–11]. Electroconvection has thus been regarded as a useful and convenient system for deep and broad research on spatiotemporal chaos. Therefore, including spatiotemporal chaos, various nonlinear phenomena in electroconvection have fascinated us for the last several decades. There has been recent research on soft-mode turbulence in a homeotropic nematic system, where the nematic director behaves as a Nambu-Goldstone mode, considering the Lagrangian picture [8,12–14] as well as the Eulerian picture [15,16]. However, there has been only limited research on spatiotemporal chaos employing the Lagrangian picture of a planar system [17]. In this paper, we report the statistical mechanical properties of spatiotemporal chaos, such as defect turbulence [see Fig. 1(a)] and spatiotemporal intermittency [see Fig. 1(b)], employing the Lagrangian picture for the planar system by measuring chaotic advection.

In response to an increase in the applied voltage V, the normal rolls (stripe pattern) become unstable and fluctuate. Because the fluctuations induce defects in the stripe pattern, this state is called defect chaos or defect turbulence [18]. The phenomenon called defect turbulence (chaos) also occurs in the complex Ginzburg-Landau equation (defect-mediated turbulence) [19] and the Rayleigh-Bénard convection (spiral defect chaos) [20]. The defect turbulence in electroconvection of nematics occurs by the different mechanism from them. Long-wavelength fluctuations in the stripe pattern are expressed by the spatiotemporal change of phase that accompanies breaking of a continuous translational symmetry with forming the stripe pattern. The defect corresponds to a singular point of the phase. In the defect turbulence in electroconvection of nematics, locally regular structures are maintained, and the correlation length corresponding to the average distance between defects is sufficiently larger than the roll size. The defect turbulence is thus a type of weak turbulence, namely spatiotemporal chaos, that occurs by weak nonlinearity [21] and has been investigated as a typical example of spatiotemporal chaos [22,23].

*hidaka@ap.kyushu-u.ac.jp

 ©2015 American Physical Society

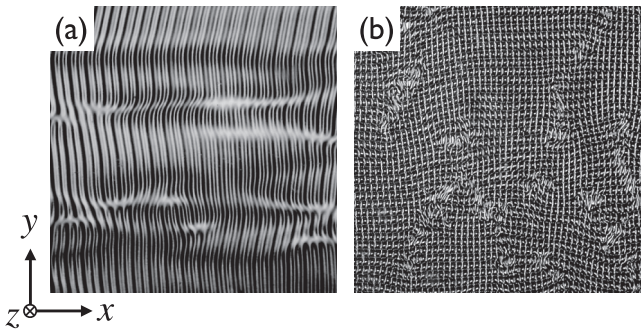

FIG. 1. Typical patterns of spatiotemporal chaos in a planar nematic system: (a) defect turbulence and (b) spatiotemporal intermittency.

The density of defects increases with an increase in V in defect turbulence. Finally, the motion of defects is frozen in portions of the system, and three-dimensional regular convection called a grid pattern (GP) appears [24]. The GP has also been studied as a research subject of nonlinear physics [25,26]. Unlike normal rolls, the GP does not appear uniformly and is localized in space [27]. GP clusters then form in the defect turbulence and coexist with the defect turbulence. The clusters dynamically change in size and shape. In other words, there is spatiotemporal intermittency, such as in ubiquitous spatiotemporal chaos [28–36], where ordered and disordered states coexist [21]. In past studies employing the Eulerian picture, area binarization analysis, which separates ordered and disordered areas, has investigated the statistics of the fraction of the ordered area to the whole area, the size distribution of clusters, and the distribution of the duration of the order or disorder state at each fixed location [31–34]. In the present research, however, we compare the properties of spatiotemporal intermittency obtained in the Lagrangian picture with those obtained in the Eulerian picture.

II. EXPERIMENT

The sample cell used in the present research was prepared by employing the standard method for the planar alignment of a nematic liquid crystal p-methoxybenzylidene-p'-n-butylaniline (MBBA) [37]. The area of the square electrodes was 1.0×1.0 cm^2, and the thickness of the cell was 67 μm. Thus, the aspect ratio of the convective system was $\Gamma = 149$. The director of the nematic liquid crystal was parallel to the x direction, and an alternating-current voltage $V_{ac}(t) = \sqrt{2}V\cos(2\pi f t)$ was applied to the sample in the z direction. In all measurements, the temperature was kept at 30.00 ± 0.03°C. The relative dielectric constant and the electric conductivity perpendicular to the nematic director of the sample cell were $\epsilon_\perp = 5.4$ and $\sigma_\perp = 3.7 \times 10^{-7}\ \Omega^{-1}\,\mathrm{m}^{-1}$, respectively. At voltages V beyond a threshold V_c, electroconvection occurred and a convective stripe pattern referred to as normal rolls appeared in the planar nematic system. The wave vector of the stripe pattern was parallel to the x direction. Hereafter, we use the normalized voltage $\varepsilon = (V^2 - V_c{}^2)/V_c{}^2$ as the control parameter. The critical frequency f_c separating the conductive regime from the dielectric regime of the electrohydrodynamic instability was obtained by fitting the frequency dependence of the convective threshold voltage V_c with the theoretical equation [38]. The present study was performed for $f = 0.65 f_c$, where $f_c = 2964$ Hz.

To observe chaotic advection, small particles (Micropearl KBS-5065, Sekisui Chemical, Osaka, Japan) were introduced into the sample cell. The diameters of the particles were 6.48 ± 0.17 μm and the density of particles was 1.22×10^3 kg/m^3, which was a little higher than that of the MBBA (1.02×10^3 kg/m^3). The x-y plane of the sample cell was observed from the z direction using a digital microscope (VHX-900, Keyence, Osaka, Japan). Time sequences of observed images $I(x,y;t)$ were stored on a magnetic disk for computer analysis. From $I(x,y;t)$, the motion of a particle $(X(t),Y(t))$ was recorded using motion analysis software (VW-H1MA, Keyence). Self-made software and ImageJ [39] were used for the analyses of $I(x,y;t)$ and $(X(t),Y(t))$.

In the measurements of the defect turbulence, two particles were observed over a period of 1800 s, and the spatial and temporal resolutions of $(X(t),Y(t))$ were 0.96 μm and 3 s/frame, respectively. Because the motion in the x direction characterizes fluctuations of the defect turbulence, we discuss only $X(t)$.

With increasing V, the GP area fraction S_g in the spatiotemporal intermittency increased and decreased, thus showing a maximum. The measurements of the spatiotemporal intermittency were made at $\varepsilon = 3.9$ (beyond the maximum) and S_g was 0.79 ± 0.05. A video was also taken for the period of 1800 s to observe both the spatial pattern and the particle motion. The spatial and temporal resolutions of $(X(t),Y(t))$ were 1.82 μm and 0.47 s, respectively. The study objects were 10 particles, and the full observation time was 10,953 s. For comparison between the Lagrangian and Eulerian pictures, a temporal sequence of images $I(x,y;t)$ was also captured. The space and time resolutions of the images were 1.82 μm/pixel and 1.0 s/frame, respectively. The size of each image was 800×480 pixels. Binarization analysis of each image $I(x,y;t)$ was conducted as follows. A partial area around an objective location was extracted from an image, and there was either GP or turbulence according to the spatial power spectrum of the area. By carrying out this process for all locations in the image, a binarized image was obtained. Dichotomous time series having length of 1800 s were obtained at 180 points of the spatial sequence. The duration (life) τ of the GP state was measured from the time series.

III. RESULTS AND DISCUSSION

A. Defect turbulence

Figure 2(a) shows $X(t)$ of a particle for $\varepsilon = 0.20$, which is slightly above the threshold of the defect turbulence. In the normal rolls with no fluctuation, the particle was trapped in a roll, and the motion showed almost only periodic oscillation owing to the circular flow of the convection. In the defect turbulence, there was hopping to the neighboring roll owing to the weak fluctuation as seen around $t = 350$ s in Fig. 2(a). For higher ε, because the convective flow is fast, particles could not follow the convective flow. The periodic motion of a particle was thus no longer observed for $\varepsilon = 0.32$ as shown in Fig. 2(b).

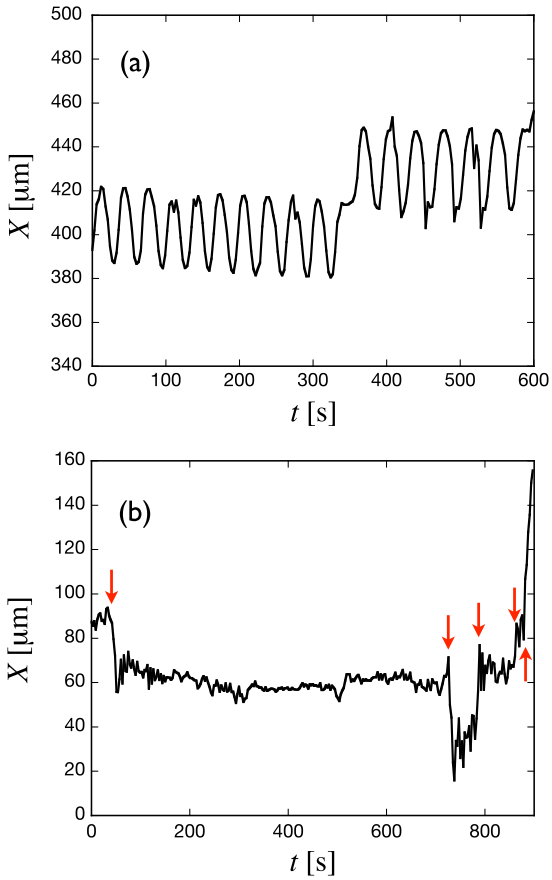

FIG. 2. (Color online) $X(t)$ of a particle for (a) $\varepsilon = 0.20$ and (b) $\varepsilon = 0.32$. The red arrows in (b) indicate hopping of the particle.

However, there were occasional large motions as indicated by the arrows in Fig. 2(b). These motions corresponded to the hopping between neighboring rolls.

The ε dependence of the hopping rate defined as the number of hops per second was measured. Because the fluctuation intensified with an increase in ε, the hopping rate also increased. We treated these data from the following viewpoint. The periodic arrangement of convective rolls in the normal rolls can be regarded as a one-dimensional periodic potential in space, and a particle trapped in a roll remains at a minimum of the potential. The defect turbulence is recognized as a fluctuation of such potential. The particle hops to the neighboring minimum in response to the fluctuation.

Generally, the hopping rate k for a potential barrier can be described by the Kramers formula:

$$k = k_0 \exp(-E/M), \tag{1}$$

where k_0 is a constant, E is the height of the potential, and M is the intensity of the fluctuation. If the hopping occurs because of thermal fluctuations, then $M = k_B T$, where k_B is the Boltzmann constant and T is the temperature. In the present case, M is an increasing function of ε that corresponds to the energy injected into the system. Experimental evidence that ε plays a similar role to that of temperature has been found for soft-mode turbulence by taking the analogy of thermal fluctuation [13,40,41]. Although the behavior of the soft-mode turbulence and that of the defect turbulence are different, the

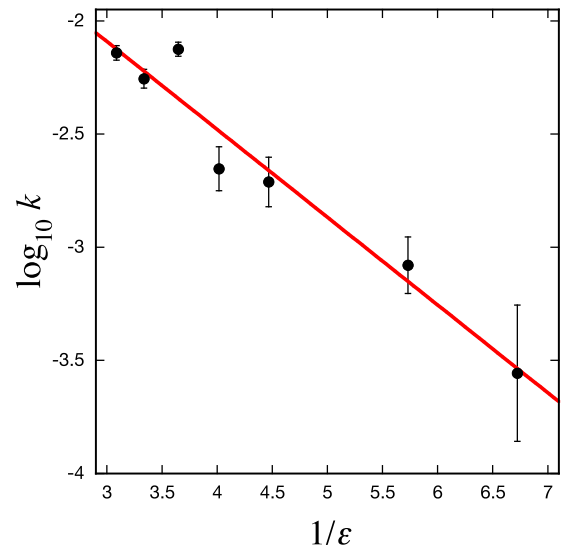

FIG. 3. (Color online) $1/\varepsilon$ versus $\log_{10} k$, where k is the hopping rate defined as the number of hops per second. The number of hops was measured over a period of 3600 s (1800 s × 2 particles).

two forms of turbulence are generated by nonlinear interaction between convection and the nematic director. Based on this common property, $M = \varepsilon$ can be supposed also in this case of the defect turbulence. In fact, $\log k$ linearly depends on $1/\varepsilon$ as shown in Fig. 3, indicating that the relation $k = k_0 \exp(-E_k/\varepsilon)$ is held. Thus, $E_k = 0.39 \pm 0.04$ is obtained from the slope of the linear relation, which corresponds to the activation energy of the potential in the unit of ε.

Each of the two time series of $X(t)$ for a period of 1800 s is divided into four, and from the eight samples, we obtain the effective diffusion constants defined as

$$D = \frac{\langle |X(T_1) - X(0)|^2 \rangle}{2T_1}, \tag{2}$$

where $\langle \cdots \rangle$ is the ensemble average of the eight samples, and $T_1 = 450$ s. The relation $D = D_0 \exp(-E_D/\varepsilon)$ is obtained as shown in Fig. 4, where D_0 is a constant. From the slope

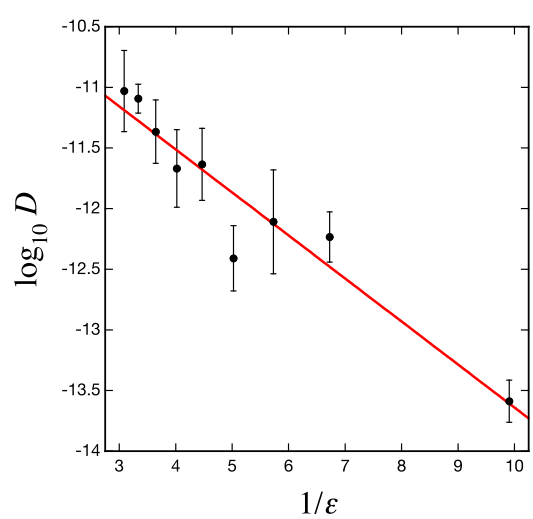

FIG. 4. (Color online) $\log_{10} D$ versus $1/\varepsilon$, where D is the diffusion constant expressed by Eq. (2).

of the linear relation shown in Fig. 4, another activation energy is obtained as $E_D = 0.35 \pm 0.04$. The relation $D = D_0 \exp(-E_D/\varepsilon)$ and $E_D \simeq E_k$ suggest that hopping plays a dominant role in the diffusion of the defect turbulence.

The concept of hopping diffusion in a periodic potential has been introduced in solid state physics [42] and biophysics [43]. However, such systems are microscopic, and the fluctuating forces are usually regarded as thermal. The present results show that this concept is available also for macroscopic convective systems with nonthermal (chaotic) fluctuations.

B. Spatiotemporal intermittency in the GP

Figure 5 show typical particle trajectories in a GP area [Figs. 5(a)–5(c)] and in a turbulent area [Figs. 5(d)–5(f)]. The particle fluctuates in a single GP cell, while it moves widely in a turbulent area. The trajectory of a particle over a period of 1800 s is shown in Fig. 6. Both stagnation in GP areas and fast motion in turbulent areas are observed; i.e., there is intermittency owing to irregular alternation between slow and fast diffusion.

To extract the property of the intermittency, the following function is proposed:

$$\Delta(t) = \frac{\{X(t+T_\Delta) - X(t)\}^2 + \{Y(t+T_\Delta) - Y(t)\}^2}{4T_\Delta}, \quad (3)$$

where T_Δ is chosen as 40 s to be sufficiently larger than the correlation time of the velocity in the turbulent area. Equation (3) therefore gives the diffusion coefficient in the period from t to $t + T_\Delta$. The comparison between $\Delta(t)$ shown in Fig. 7 and the observation of particle motion reveals that the particle was located in GP areas when $\Delta(t)$ was relatively small and in turbulent areas when $\Delta(t)$ was relatively large. In the spatiotemporal intermittency, therefore, the diffusion coefficient should be described not as a constant but as a spatiotemporal variable.

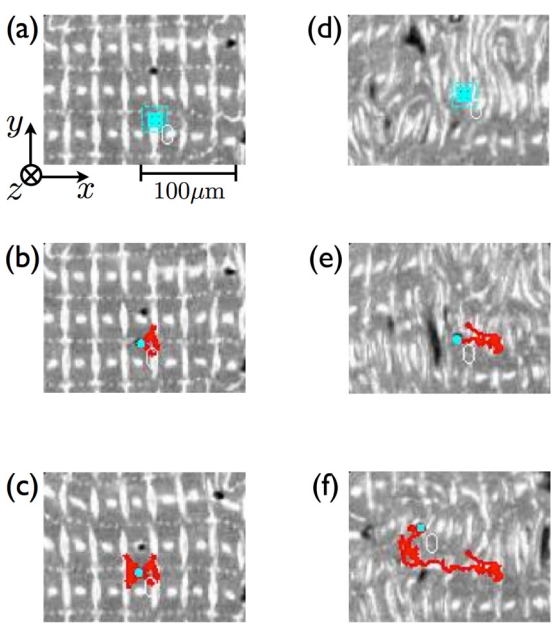

FIG. 5. (Color online) Typical particle trajectories in (a–c) a grid area and (d–f) a turbulent area. The blue dots and red lines indicate the position at t and trajectory from 0 s to t, respectively. (a, d) $t = 0$ s; (b, e) $t = 10$ s; (c, f) $t = 20$ s.

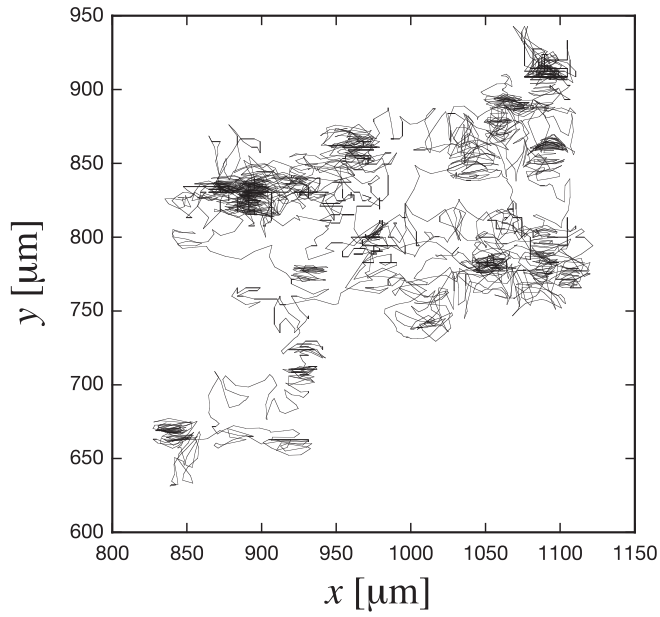

FIG. 6. Trajectory of a particle over a period of 1800 s in the spatiotemporal intermittency.

$\Delta(t)$ can be binarized as well as GP and turbulent areas. To do so, the average value $\bar{\Delta}$ of $\Delta(t)$ is used as a threshold. From the binarized time series, we obtain the distribution function $P_L(\tau)$ of the duration τ in which a particle exists in a GP area. Thus, $P_L(\tau)$ in the Lagrangian picture well fits a power-law function as shown in Fig. 8.

Let us compare the above result with that of the Eulerian picture. The distribution function $P_E(\tau)$ of the duration time obtained from the area binarization analysis well fits a power-law function with an index 1.53 ± 0.04 as shown in Fig. 9 in the Eulerian picture. Thus, both cases well fit a similar power law $\tau^{-\eta}$ but with $\eta_L = 1.00 \pm 0.06$ for $P_L(\tau)$ and $\eta_E = 1.53 \pm 0.04$ for $P_E(\tau)$. In the Lagrangian picture, because both random particle motions and pattern dynamics are simultaneously effective, the particles are rarely able to stay at the same area and are driven to move away. Therefore, $P_L(\tau)$ tends to decrease more quickly than $P_E(\tau)$ for long τ. Thus, we expect that η_L is larger than η_E. However, our observation

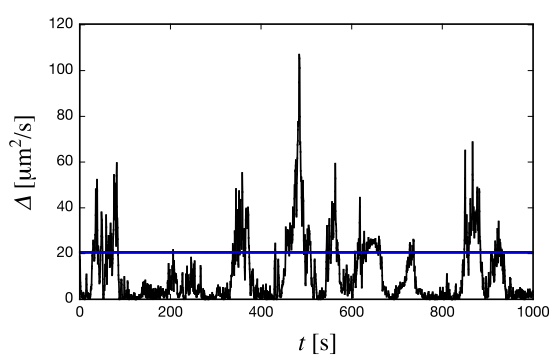

FIG. 7. (Color online) $\Delta(t)$ defined by Eq. (3). The blue line indicates $\bar{\Delta}$.

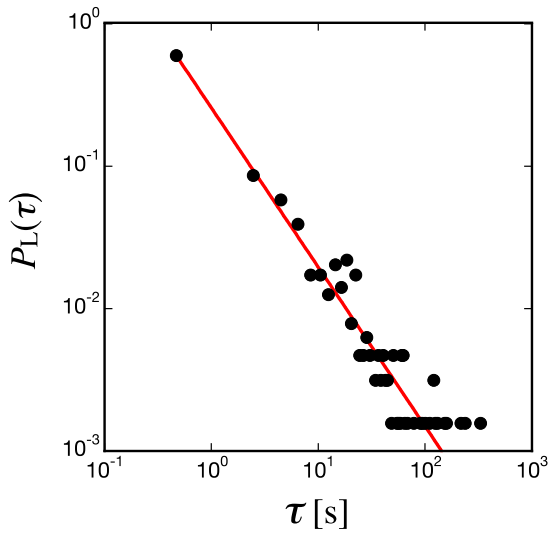

FIG. 8. (Color online) Distribution function $P_L(\tau)$ of the duration in which a particle exists in a grid area.

disagrees with the expectation. This can be explained by tracing a single particle as follows. A turbulent domain appears to flick a particle as if there is a wall, and a particle therefore stays longer in an ordered state. In addition, even if a particle can enter a turbulent domain, the particle only ever stays for a very short time because of flicking from the turbulent regimes. The particle thus stays longer in ordered states, and the lifetime in the Lagrangian picture is longer. In other words, less mixing for long τ is observed in the Lagrangian picture than in the Eulerian picture. This explains why η_L is smaller than η_E.

There has been much research on spatiotemporal intermittency by analogy with percolation, especially directed percolation that includes temporal development [31–34]. The critical behavior of statistics such as the size distribution of the ordered domain has been investigated. Similar to the case of directed percolation [44], the distribution function has a power-law decay only at a critical point. In the present research, however,

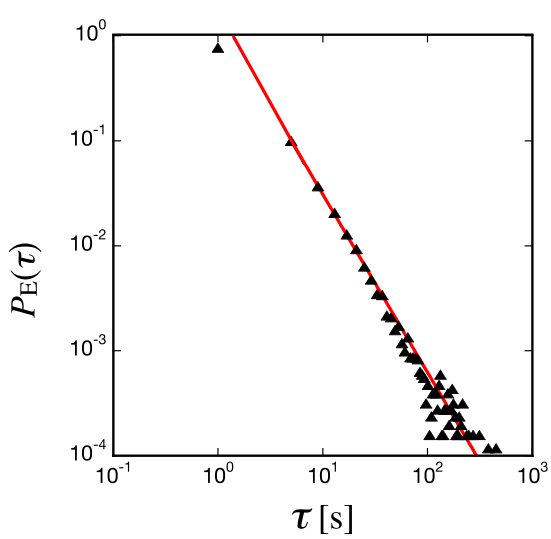

FIG. 9. (Color online) Distribution function $P_E(\tau)$ of the duration of the ordered state.

it is thought that the distribution function of the ordered state has a power-law decay in a wide range of ε, because our case $\varepsilon = 3.9$ is not a critical point but rather a normal point. This behavior is a kind of "generic scale invariance" that is characteristic of spatiotemporal chaos [45]. The GP is a spatially ordered pattern that appears reentrantly from the defect turbulence and contains background macrofluctuations. These chaotic fluctuations may break the order partially; consequently, the spatiotemporal intermittency is enhanced. As mentioned in Ref. [45], the reason for the generic scale invariance may be that the noise that induces a transition between ordered and disordered states is not of thermal origin but of nonthermal origin, i.e., deterministic chaos. Such nonthermal fluctuations should have long-wavelength and long-time correlation that may induce the critical behavior. However, the detail of the critical behavior has not yet been clarified.

IV. SUMMARY

The properties of spatiotemporal chaos in the electroconvection of a planar alignment system of a nematic liquid crystal were investigated from the viewpoint of the Lagrangian picture. In the defect turbulence, a particle that was trapped in a convective roll rarely hopped to a neighboring roll. Making the assumption that the strength of fluctuations in the Kramers formula for the hopping rate is proportional to ε, the activation energy for transition from one convective roll to another was obtained from the ε dependence of the hopping rate. The activation energy was also obtained directly from the diffusion coefficient of particle motions using another method. The two activation energies were almost the same, suggesting that hopping diffusion was dominant in the defect turbulence.

We finally summarize our observations of the spatiotemporal intermittency made in the present study. There is a clear boundary between the GP domain and defect turbulence domain. The boundary randomly moves and the domains therefore dynamically change in space and time. Because of this boundary motion, there is intermittent switching of low diffusion velocity in a GP area and high diffusion velocity in a turbulent area. This particle diffusion can be regarded as a Lagrangian process. Because of this switching, the distribution of the duration in which a particle exists in a grid area follows a power law. This result shows that intermittent switching between low and high diffusion velocities is not a Poisson process and may indicate a type of critical state. Moreover, the distribution function of the lifetime of ordered GP patterns, like that in the Eulerian picture, follows a power law. The two functions can be described by similar power laws; nevertheless, the index of the power law is 1.00 ± 0.06 in the Lagrangian picture and 1.53 ± 0.04 in the Eulerian picture. This difference suggests different dynamics, which are presently unknown, in the two pictures.

ACKNOWLEDGMENTS

We thank Masaru Suzuki and Takayuki Narumi for helpful comments and discussions. This work was supported by JSPS KAKENHI Grant Nos. 21340110, 21540391, 24540408, and 15K05799.

[1] M. C. Cross and P. C. Hohenberg, Rev. Mod. Phys. **65**, 851 (1993).
[2] A. S. Monin and A. M. Yaglom, *Statistical Fluid Mechanics*, edited by J. L. Lumley, Mechanics of Turbulence (MIT Press, Cambridge, MA, 1971).
[3] P. C. Hohenberg and B. I. Shraiman, Physica D **37**, 109 (1989).
[4] H. Aref, J. Fluid Mech. **143**, 1 (1984).
[5] T. H. Solomon and J. P. Gollub, Phys. Rev. A **38**, 6280 (1988).
[6] J. M. Ottino, *The Kinematics of Mixing* (Cambridge University Press, Cambridge, U.K., 1989).
[7] *Transport and Mixing in Geophysical Flows*, edited by J. B. Weiss and A. Provenzale (Springer-Verlag, Berlin, 2008).
[8] K. Tamura, Y. Yusuf, Y. Hidaka, and S. Kai, J. Phys. Soc. Jpn. **70**, 2805 (2001).
[9] S. Kai and W. Zimmermann, Prog. Theor. Phys. Suppl. **99**, 458 (1989).
[10] M. Dennin, G. Ahlers, and D. S. Cannell, Science **272**, 388 (1996).
[11] Y. Hidaka, K. Tamura, and S. Kai, Prog. Theor. Phys. Suppl. **161**, 1 (2006).
[12] K. Tamura, Y. Hidaka, Y. Yusuf, and S. Kai, Physica A **306**, 157 (2002).
[13] Y. Hidaka, Y. Hosokawa, N. Oikawa, K. Tamura, R. Anugraha, and S. Kai, Physica D **239**, 735 (2010).
[14] M. Suzuki, H. Sueto, Y. Hosokawa, N. Muramoto, T. Narumi, Y. Hidaka, and S. Kai, Phys. Rev. E **88**, 042147 (2013).
[15] R. Anugraha, K. Tamura, Y. Hidaka, N. Oikawa, and S. Kai, Phys. Rev. Lett. **100**, 164503 (2008).
[16] T. Narumi, J. Yoshitani, M. Suzuki, Y. Hidaka, F. Nugroho, T. Nagaya, and S. Kai, Phys. Rev. E **87**, 012505 (2013).
[17] K. Takahashi and Y. Kimura, Phys. Rev. E **90**, 012502 (2014).
[18] S. Kai, N. Chizumi, and M. Kohno, J. Phys. Soc. Jpn. **58**, 3541 (1989).
[19] P. Coullet, L. Gil, and J. Lega, Phys. Rev. Lett. **62**, 1619 (1989).
[20] S. W. Morris, E. Bodenschatz, D. S. Cannell, and G. Ahlers, Phys. Rev. Lett. **71**, 2026 (1993).
[21] Y. Hidaka and N. Oikawa, FORMA **29**, 29 (2014).
[22] L. Silvestri, L. Fronzoni, P. Grigolini, and P. Allegrini, Phys. Rev. Lett. **102**, 014502 (2009).
[23] P. Allegrini, M. Bologna, L. Fronzoni, P. Grigolini, and L. Silvestri, Phys. Rev. Lett. **103**, 030602 (2009).
[24] S. Kai and K. Hirakawa, Prog. Theor. Phys. Suppl. **64**, 212 (1978).
[25] S. Kai, H. Fukunaga, and H. R. Brand, J. Stat. Phys. **54**, 1133 (1989).
[26] T. Kawagishi, T. Mizuguchi, and M. Sano, Phys. Rev. Lett. **75**, 3768 (1995).
[27] S. Hirata and T. Tako, J. Phys. Soc. Jpn. **51**, 2405 (1982).
[28] K. Kaneko, Prog. Theor. Phys. **74**, 1033 (1985).
[29] Y. Pomeau, Physica D **23**, 3 (1986).
[30] H. Chaté and P. Manneville, Phys. Rev. Lett. **58**, 112 (1987).
[31] S. Ciliberto and P. Bigazzi, Phys. Rev. Lett. **60**, 286 (1988).
[32] F. Daviaud, M. Bonetti, and M. Dubois, Phys. Rev. A **42**, 3388 (1990).
[33] M. Caponeri and S. Ciliberto, Physica D **58**, 365 (1992).
[34] M. M. Degen, I. Mutabazi, and C. D. Andereck, Phys. Rev. E **53**, 3495 (1996).
[35] N. Oikawa, Y. Hidaka, and S. Kai, Prog. Theor. Phys. Suppl. **161**, 320 (2006).
[36] N. Oikawa, Y. Hidaka, and S. Kai, Phys. Rev. E **77**, 035205 (2008).
[37] N. Oikawa, Y. Hidaka, and S. Kai, Phys. Rev. E **70**, 066204 (2004).
[38] E. Dubois-Violette, P. G. de Gennes, and O. Parodi, J. Phys. France **32**, 305 (1971).
[39] C. A. Schneider, W. S. Rasband, and K. W. Eliceiri, Nat. Methods **9**, 671 (2012).
[40] S. Kai, K.-i. Hayashi, and Y. Hidaka, J. Phys. Chem. **100**, 19007 (1996).
[41] K. Tamura, R. Anugraha, R. Matsuo, Y. Hidaka, and S. Kai, J. Phys. Soc. Jpn. **75**, 063801 (2006).
[42] W. Dieterich, I. Peschel, and W. R. Schneider, Z. Phys. B **27**, 177 (1977).
[43] P. Reimann, Phys. Rep. **361**, 57 (2002).
[44] K. A. Takeuchi, M. Kuroda, H. Chaté, and M. Sano, Phys. Rev. Lett. **99**, 234503 (2007).
[45] B. W. Roberts, E. Bodenschatz, and J. P. Sethna, Physica D **99**, 252 (1996).